

Comparing Anthropometric and Quality Assurance Phantoms in Quantitative Image Quality Testing for CBCT Imaging

KIBT Görüntüleme Kantitatif Görüntü Kalitesi Testleri İçin Antropometrik ve Kalite Güvence Fantomlarının Karşılaştırılması

Hakan Amasya¹, Şelale Özel², Duygu Tunçman Kayaokay³,
Songül Çavdar Karaçam⁴, Kaan Orhan⁵, Mustafa Demir⁶

ABSTRACT

Aim: This study aims to imaging an anthropometric phantom and a quality assurance (QA) phantom with cone-beam computed tomography (CBCT) in three different dose protocols and to compare the quantitative image quality test values calculated with the anthropometric phantom with the QA phantom results in selected slices. Thus, it is aimed to produce information regarding the validity of image quality tests performed with anthropometric phantom slices.

Materials and Method: Alderson-Rando® phantom (Radiology Support Devices, Long Beach, CA) and QA phantom (QR Verona, Italy) were imaged with a MyRay Hyperion X9 Pro (Cefla, Imola, Italy) KIBT device. The field of view was chosen as 13x10 cm and three different imaging modes (Low Dose, Normal, High Quality) were implemented while keeping other parameters constant. Three slices were selected from the anthropometric phantom volumes (paranasal sinus, maxilla, mandible) and one slice from the QA phantom. A total of 12 image samples were imported into ImageJ software for signal-to-noise ratio and contrast-to-noise ratio calculations. Differences between three or more variables (Low Dose, Normal, High Quality, or paranasal sinus, maxilla, mandible and QA phantom slices) were evaluated by Kruskal-Wallis test, while the relationship between pairs of variables was analyzed by Spearman and Kendall's rank correlation coefficient. The statistical significance threshold was set as $p < 0.05$.

Results: The differences between the selected slices (paranasal sinus, maxilla, mandible, QA) and imaging modes (Low Dose, Routine, High Quality) were both statistically insignificant. According to Spearman's ρ , the correlation between QA phantom and maxillary and mandibular slices was statistically significant. SNR values for maxillary and mandibular slices were calculated between 12.6 and 23.1 for anthropometric phantom slices and between 16.2 and 23.3 for QA phantom slices. The CNR values were between 13.2 and 88.5 for the respective anthropometric phantom slices and 15.5 and 20.6 for the QA phantom.

Conclusion: The results of this study support that the measurements made with anthropometric phantom slices for image quality testing in CBCT are similar to those made with the QA phantom in the maxilla and mandible regions. Future studies with different phantom types, imaging systems and radiographic parameters may be considered to produce information about the advantages and disadvantages of the two phantom types in image quality testing.

Keywords: Cone-beam computed tomography; Quality control; Radiology

ÖZET

Amaç: Bu çalışmanın amacı, bir antropometrik fantom ve bir kalite güvence (KG) fantomunun konik-ışınli bilgisayarlı tomografi (KIBT) ile üç farklı doz protokolünde görüntülenmesi ve seçilen kesitlerde antropometrik fantom ile hesaplanan kantitatif görüntü kalitesi testi değerlerinin KG fantomu sonuçlarıyla kıyaslanmasıdır. Böylece, antropometrik fantom kesitleriyle yapılan görüntü kalitesi testlerinin geçerliliği hakkında bilgi üretimi hedeflenmektedir.

Gereç ve Yöntem: Alderson-Rando® fantomu (Radiology Support Devices, Long Beach, Kaliforniya) ve KG fantomu (QR Verona, İtalya) MyRay Hyperion X9 Pro (Cefla, Imola, İtalya) KIBT cihazı ile görüntüldü. Görüş alanı 13x10 cm olarak seçildi ve diğer parametreler sabit tutulurken üç farklı görüntüleme modu (Düşük Doz, Normal, Yüksek Kalite) uygulandı. Antropometrik fantom hacimlerinden üçer kesit (paranasal sinüs, maksilla, mandibula) ve KG fantomundan bir kesit seçildi. Toplam 12 görüntü örneği sinyal-gürültü oranı ve kontrast-gürültü oranı hesaplamaları için ImageJ yazılımına aktarıldı. Üç ve daha fazla değişken (Düşük Doz, Normal, Yüksek Kalite, veya paranasal sinüs, maksilla, mandibula ve KG kesitleri) arasındaki farklar Kruskal-Wallis testi ile değerlendirilirken sürekli değişken çiftleri arasındaki ilişki Spearman ve Kendall'ın sıra korelasyon katsayısı ile analiz edildi. İstatistiksel anlamlılık eşiği $p < 0.05$ olarak belirlendi.

Bulgular: Seçilen kesitler (paranasal sinüs, maksilla, mandibula, KG) ve görüntüleme modları (Düşük Doz, Rutin, Yüksek Kalite) arasındaki farkların her ikisi de istatistiksel olarak anlamsız bulundu. Spearman's ρ göre, KG fantomu ile maksiller ve mandibular kesitler arasındaki ilişki istatistiksel olarak anlamlı bulundu. Maksilla ve mandibula kesitleri için SNR değeri, antropometrik fantom kesitlerinde 12.6-23.1 arasında, KG fantomda ise 16.2-23.3 arasında hesaplandı. CNR değeri ise, ilgili antropometrik fantom kesitlerinde 13.2-88.5 arasında, KG fantom için ise 15.5-20.6 arasında bulundu.

Sonuç: Bu çalışmanın sonuçları, KIBT'de görüntü kalitesi testi için antropometrik fantom kesitleri ile yapılan ölçümlerin KG fantomu ile yapılanlara maksilla ve mandibula bölgelerinde benzer olduğunu destekler. İleride farklı fantom tipleri, görüntüleme sistemleri ve radyografik parametrelerle yapılacak çalışmalarla, görüntü kalitesi testlerinde iki fantom tipinin avantaj ve dezavantajları hakkında bilgi üretimi düşünülebilir.

Anahtar Kelimeler: Kalite kontrol; Konik-ışınli bilgisayarlı tomografi; Radyoloji

Makale gönderiliş tarihi: 11.09.2024; Yayına kabul tarihi: 08.03.2025

İletişim: Dr. Hakan Amasya

İstanbul Üniversitesi Cerrahpaşa Diş Hekimliği Fakültesi Cerrahpaşa Yerleşkesi Kocamustafapaşa Caddesi No:53 Cerrahpaşa 34098 Fatih, İstanbul, Türkiye

E-mail: hakanamasya@iuc.edu.tr

¹ Asst.Prof., Department of Oral and Dentomaxillofacial Radiology, Faculty of Dentistry, Istanbul University-Cerrahpaşa, Istanbul, Türkiye

² Asst.Prof., Department of Oral and Dentomaxillofacial Radiology, Faculty of Dentistry, Altınbaş University, Istanbul, Türkiye

³ Asst.Prof., Radiotherapy Program, Vocational School of Health Services, Istanbul University-Cerrahpaşa, Istanbul, Türkiye

⁴ Assoc. Prof., Radiotherapy Program, Vocational School of Health Services, Istanbul University-Cerrahpaşa, Istanbul, Türkiye

⁵ Prof., Department of Dentomaxillofacial Radiology, Faculty of Dentistry, Ankara University, Ankara, Türkiye

⁶ Prof., Department of Nuclear Medicine, Cerrahpaşa Faculty of Medicine, Istanbul University-Cerrahpaşa, Istanbul, Türkiye

INTRODUCTION

Cone-beam computed tomography (CBCT) is a technique commonly used in dentistry for diagnosis and treatment planning, as well as in interventional radiology and radiotherapy. For image quality tests on the relevant devices, common tests can be applied for different device types, and specific tests may be required depending on the device type and purpose.¹ Quality assurance (QA) guidelines for CBCT include recommendations on principles of use, indications, dose optimization, commissioning, and periodic testing. Specific QA phantoms are often required for quantitative image quality testing. However, the need for improvement in QA phantoms for CBCT imaging is discussed in the literature. Although phantoms produced for computed tomography (CT) are commonly used in image quality assessment, this has limitations in tests requiring higher resolution and simulation of metal artifacts. In addition, CT phantoms for soft tissue have limited utility in CBCT. Overall, there is a need for a universal CBCT QA phantom that can be used in different CBCT devices and with which test results can be compared.¹⁻⁴

Recent studies have assessed various image quality parameters such as artifacts, spatial resolution, image uniformity, and geometric accuracy using different types of phantoms, including water phantoms, manufacturer-provided phantoms, and phantoms developed by researchers. Polymethyl methacrylate (PMMA) phantoms, in particular, have been recognized as effective tools in image quality testing. However, not all developed phantoms meet the strict criteria required for comprehensive quality assessment, highlighting the ongoing need for innovation in phantom design.⁴⁻⁶

An anthropometric phantom is made of synthetic material that simulates the human anatomy and tissue composition in slices. It is used in dose calculations in radiation practices by placing dosimetry equipment in the holes formed in the slices. After physically simulating the relevant radiation application using phantoms, the measurements of dosimetry equipment are calculated, and these data are evaluated for risk calculation and dose optimization.⁷⁻¹⁰ In diagnostic imaging studies, radiographic data acquisition, which represents the internal composition of the anthropometric phantom, is performed during

the experiment.¹¹ Although QA phantoms are routinely used for image quality testing, the question of whether the volumes acquired with an anthropometric phantom can be used in similar image testing may be worth investigating.

This study aims to compare the quantitative image quality tests conducted with anthropometric and QA phantom in dental CBCT imaging. The null hypothesis is that the difference between the quantitative image quality tests performed with anthropometric phantom and QA phantom is statistically significant. Rejection of the null hypothesis can be considered to support the suggestion that the two phantoms are interchangeable in CBCT for image quality tests with limitations of each type.

MATERIAL AND METHOD

In this study, an anthropometric phantom and a QA phantom were imaged with a dental CBCT device in three different imaging protocols, namely "Low Dose," "Regular" and "Best Quality" modes, and quantitative image quality tests were performed on selected slices to be compared. Ethics committee approval was not obtained as this study did not involve human subjects.

Preparing the Samples

The Alderson-Rando® phantom (Radiology Support Devices, Long Beach, CA) simulating an average adult female (155 cm, 50 kg) was used to imitate soft and hard tissues (Figure 1). The first twelve of the horizontally oriented slices (2.5 cm thick) representing the head and neck region were fixed with nylon rods passing through the edges of the center section. Dosimetry equipment was not placed, and the top aluminum plate was not attached to avoid the metal artifacts. During imaging, a natural spine posture in phantom position and a Frankfort horizontal plane parallel to the ground were verified. Chin and head fixation apparatus were used to stabilize the phantom's head, whereas the bite stick was not employed. The QA phantom (QR Verona, Italy) which contains aluminum cylinder inside (Figure 2) was used as the control phantom. Both the anthropometric phantom and the QA phantom were placed on a BS-500 adjustable monitor stand (Millenium, Treppendorf, Germany) to reach the gantry. The QA phantom was raised for an extra ten cm with a card-

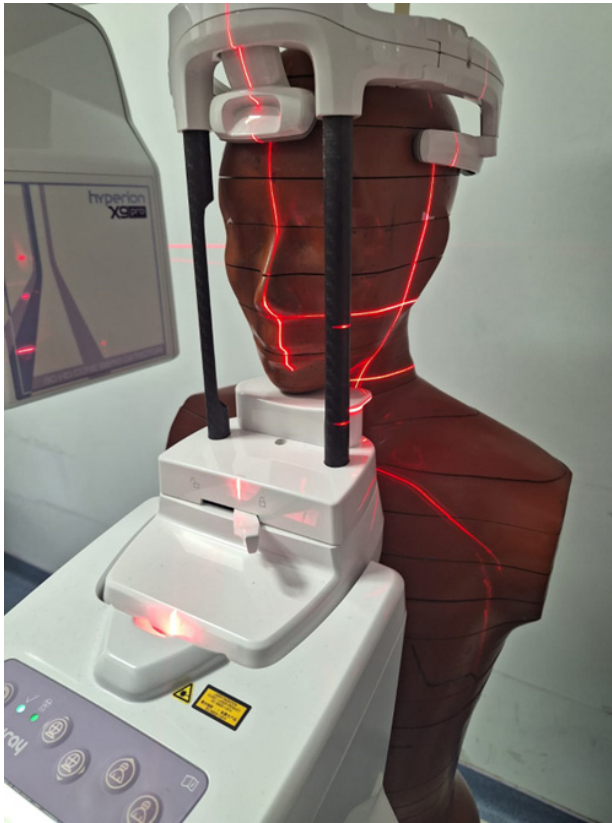


Figure 1. The Alderson-Rando® phantom (Radiology Support Devices, Long Beach, CA) is molded of tissue-equivalent material and routinely used for organ dosimetry measurements. In this study, slices selected from the volume reconstructed with CBCT irradiation were used for quantitative image quality tests.

board box to move away from the metal surface of the supporting platform. The position of the phantoms was visually checked using the Class I (IEC 60825-1:2014) laser.

Radiographic Volume Acquisition

The MyRay Hyperion X9 Pro (Cefla, Imola, Italy) CBCT machine with tele-radiographic/cephalometric arm was operated with 230V and 50 Hz electrical input (CEI OPX/105-12, IEC 60336). The X-ray was generated at 90 kVp ($\pm 5\%$) fixed pulsed beam, and mA was modulated in real-time with Automatic Morphology Recognition Technology (MRT) during volume acquisition. Field of View (FOV) was set to 13x10 cm (diameter x height) in all volume acquisitions, and vertical stitching was not required. The anthropometric phantom and QA phantom were imaged by using three different protocols: “Low Dose”

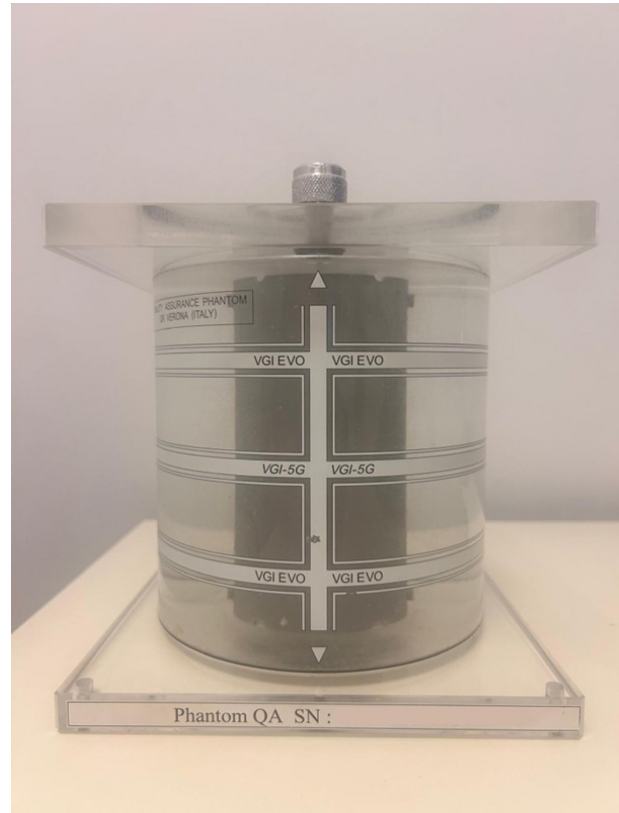


Figure 2. The QA phantom (QR Verona, Italy) which contains aluminum cylinder inside was used as the control phantom.

as 12.96 s (2.4 s exposure time), “Regular” as 14.4 s (3.6 s exposure time) and “Best Quality” as 16.8 s (5.2 s exposure time) rotation time. The amorphous silicon/cesium iodide flat panel detector was used for radiation acquisition. The signal was transferred to the HP Z2 Tower G4 Workstation (Intel® Xeon® E-2174G, 16 GB RAM, AMD Radeon Pro WX3100 (4 GB GDDR5, 10-bit) GPU) after 16-bit (65.535 gray levels) analog-to-digital conversion and volumes are reconstructed with the iRYS v15.0 software. For the three different imaging protocols, three axial slices representing the mandible, maxilla, and paranasal sinus regions were selected in the anthropometric phantom volumes, whereas in the QA phantom, a single slice with a clearly visible radiopaque layer was selected (Figure 3). Selected slices were exported in DICOM format and prepared for image quality tests.

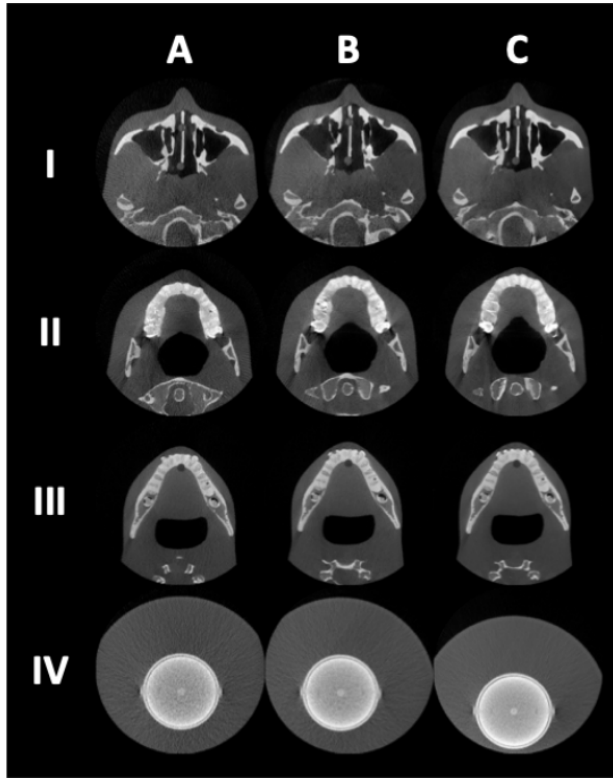


Figure 3. CBCT slices selected for image quality tests. I: Paranasal Sinus, II: Maxilla, III: Mandible, IV: Quality Assurance Phantom. A: Low Dose, B: Regular, C: Best Quality

Quantitative Image Quality Tests

The samples were imported to the ImageJ software, and three circular regions-of-interest (ROIs) 3x3 mm in size were selected to represent two contrast regions: the bone and the soft tissue. The size of the ROI was determined as the largest possible area, excluding other tissues when sampling bone and soft tissue regions in all slices. The ROIs were jointly selected by two dentomaxillofacial radiologists with nearly 10 years of experience, while randomly and equally distributed samples were validated by more experienced experts in dentomaxillofacial radiology, radiation oncology medical physics and nuclear medicine and medical imaging. The mean gray value in each ROI was combined with two other ROIs representing the relevant site to calculate the mean and standard deviations for bone and soft tissue for three different imaging protocols, at three different vertical heights on anthropometric phantoms, and on a single slice of the QA phantom. Signal-to-noise (SNR) and contrast-to-noise (CNR) values were calculated using the following formulas in MS Excel.^{2,3}

$$\text{SNR} = \frac{\text{MGV (bone)}}{\text{SD (soft tissue)}} \quad (1)$$

$$\text{CNR} = \frac{\text{MGV (bone)} - \text{MGV (soft tissue)}}{\text{SD (soft tissue)}} \quad (2)$$

MGV: Mean gray value, SD: Standard deviation

Statistical Analysis

The fit to normal distribution was assessed by the Shapiro-Wilk test. Non-parametric tests were chosen when the normality assumption was not met. The Wilcoxon Signed Rank Test was used to assess whether the mean ranks of SNR and CNR differ significantly. The Kruskal-Wallis test was performed to compare the median scores of three or more independent groups (Low Dose, Regular, and Best Quality; or Paranasal Sinus, Maxilla, Mandible, and QA Phantom). The Friedman Test was used to compare the measures of scores across three anatomical regions (Paranasal Sinus, Maxilla, and Mandible). Spearman's rank correlation coefficient (ρ) was used to assess the strength and direction of the monotonic relationship (2-tailed) between two variables: phantom and anthropometric phantom slices. Kendall's rank correlation coefficient (τ) was also performed to further validate the association between the QA phantom and the anatomical slices. Statistical significance threshold was determined as $p < 0.05$.

RESULTS

According to the MRT results, for anthropometric phantom experiments, the mAs value was determined as 7 (3 mA) in "Low Dose", 11 (3 mA) in "Regular" and 24 (4 mA) in "Best Quality" modes. For the QA phantom, the mAs value was determined as 7 (3 mA) in "Low Dose", 14 (4 mA) in "Regular" and 36 (7 mA) in "Best Quality" modes.

The Wilcoxon Signed Rank Test showed that the differences between SNR and CNR values were statistically significant ($p=0.03$). The Kruskal-Wallis test revealed that differences in SNRs and CNRs among paranasal sinus, maxilla, mandible, and QA slices ($p=0.39$) or imaging protocols ($p=0.37$) were not statistically significant (Table 1). Accordingly, the lowest measurements calculated on the QA phantom (SNR=16.2, CNR=15.5) were obtained

in the “Low Dose” protocol, while the highest values (SNR=23.3, CNR=20.6) were calculated in the “Best Quality” mode. “Regular” mode was found to be in between (SNR=19.1, CNR=17.6) the other two protocols. In the anthropometric phantom slices, a gradual increase was observed in the maxillary slices (SNR=12.6, 37.6, 97.0; CNR=13.2, 35.3, 88.5), while measurements in other regions showed an increase or decrease in different variables depending on the imaging protocol.

The Friedman test showed that the differences in SNRs or CNRs among anthropometric slices (paranasal sinus, maxilla, and mandible) for each imaging protocol were statistically significant (p=0.05). Among the anthropometric phantom slices, the lowest SNR (8.1-8.6) and CNR (8.0-8.7) values were calculated in paranasal slices, while the highest calculations were obtained in maxilla slices, except for the “Low Dose” protocol. In the “Low Dose” protocol, the highest SNR (19.1) and CNR (19.3) values were calculated in mandible slices.

Spearman’s ρ revealed that the pairwise relationships between the QA phantom and the maxillary (p=0.01), and mandibular (p=0.05) slices were statistically significant for both the SNR and CNR values, while it was found not statistically significant for QA phantom and the paranasal slices (p=0.17). Kendall’s τ revealed that only the pairwise relationship between the QA phantom and maxillary (p=0.02) slices was statistically significant, however, correlations between the QA phantom and paranasal sinus (p=0.13) or mandibular (p=0.06) slices did not reach statistical significance threshold. Among the anthropometric phantom slices, the maxilla region showed the greatest change by imaging protocol (p<0.05), while the relationships between the maxillary slices (SNR: 12.6 - 97, CNR: 13.2 - 88.5) and QA phantom (SNR: 16.2 - 23.3, CNR: 15.5 - 20.6) were found to be statistically significant (p<0.05) (Table 1).

Table 1. Signal-to-noise (SNR) and contrast-to-noise ratios (CNR) calculated using three slices of the anthropometric phantom (paranasal sinus, maxilla, and mandible) and a single slice of the quality assurance (QA) phantom.

Sample Image Slice	Signal-to-Noise Ratio				Contrast-to-Noise Ratio				p ¹	
	Low Dose	Regular	Best Quality	p ²	Low Dose	Regular	Best Quality	p ²		
Anthropometric Phantom	Paranasal Sinus	8.1	8.6	8.5	0.37	8.0	8.6	8.7	0.37	0.028*
	Maxilla	12.6	37.6	97.0	0.37	13.2	35.3	88.5	0.37	0.028*
	Mandible	19.1	19.4	23.1	0.37	19.3	19.2	23.1	0.37	0.028*
	p ³	0.046*	0.046*	0.046*		0.046*	0.046*	0.046*		
Quality Assurance Phantom	Single	16.2	19.1	23.3	0.37	15.5	17.6	20.6	0.37	0.028*
	p ²	0.39	0.39	0.39	0.39	0.39	0.39	0.39		

p¹: Wilcoxon Signed Rank Test, p²: Kruskal-Wallis Test, p³: Friedman Test

DISCUSSION

In this study, an anthropometric phantom and a QA phantom were imaged with the CBCT system in three different protocols (Low Dose, Regular, and Best Quality), and a total of six volumetric data sets were acquired. Three axial slices (paranasal sinus, maxilla, and mandible) were sampled from the anthropometric phantom volume, while a single axial slice was taken from the QA phantom volume for each imaging protocol. In each slice, three ROIs representing bone and soft tissues were identified, and SNR and CNR values were calculated by combining the mean gray values.

According to the results of this experiment, the differences in slices of paranasal sinus, maxilla, mandible, and QA were found to be statistically insignificant, while the association between QA and maxilla slices was statistically significant. The relationship between the QA and mandible slices was statistically significant with Spearman's test. There was no relationship between QA and paranasal sinus slices. Results of this study support the suggestion that the SNR and CNR values calculated in CBCT imaging using anthropometric and QA phantoms may be considered similar, but testing whether anthropometric phantom measurements can completely replace the quality control phantom was beyond the scope of the present study. Each phantom type is designed for its own purpose, and outlier measurements can be considered a secondary finding.

A study evaluated the effective dose and image quality of horizontal CBCT in comparison with multislice spiral CT (MSCT) in scans of the head, cervical spine, ear, and dental arches, which used a head and neck Alderson-Rando® phantom for effective dose calculation, while a CATPHAN® 504 phantom (The Phantom Laboratory, New York, USA) for quantitative image quality assessment concluded that in ear and dental arch imaging, CBCT was preferable to MSCT due to its lower radiation dose, and MSCT should be recommended when a high contrast resolution is required.¹² Another study compared the effective dose and subjective image quality of temporomandibular joint examinations with a dental CBCT device, a MSCT device, and an anthropometric phantom. Four dentomaxillofacial radiologists assessed the image quality on a one to three scale,

and the dose is optimized based on the scores. The authors reported a 50% dose reduction when compared to the manufacturer's standards.¹³ In the present study, radiation dose was not calculated and only CBCT was used as the imaging technique.

Ten clinically applied protocols were investigated in a study using the CS 9300 (CareStream SM 749, Rochester, NY) CBCT scanner and the CBCT QAT phantom (Kodak, Rochester, NY). The authors reported that increasing kVp results in an increase in both SNR and CNR values.¹⁴

In the present study, an increase in SNR and CNR values with increasing dose was observed in QA phantom and maxillary slices, while for paranasal and mandibular slices, minimal decreases in image quality test values were noted with increasing dose in specific conditions.

In a study evaluating image quality, segmentation accuracy, and radiation dose of four CBCT scanners, Accuitomo 3D (Morita, Kyoto, Japan), MercuRay (Medico Technology Corporation, Kashiwa, Japan), NewTom 3G (Quantive Radiology, Verona, Italy), i-CAT (Imaging Sciences International, Hatfield, PA), and a Sensation 16 (Siemens, Erlangen, Germany) multidetector computed tomography (MDCT) device, a skull phantom (scanned by laser scanner), and contrast phantom (PMMA cylinder with cylindrical inserts of air, bone, and PMMA) was used. The authors reported that the lowest radiation dose was found for the Accuitomo 3D, with the smallest image area, and the best segmentation accuracy was found for the i-CAT.¹⁵ In that study, CBCT volumes obtained with different devices were analyzed for patient dose and 3D model generation, whereas in our study, different acquisition modes on a single device were utilized.

Another study investigated the effect of mAs reduction on clinical and technical image quality using a polymethyl methacrylate (PMMA) phantom and an anthropometric skull. The PMMA phantom was used to calculate the CNR, and eight axial and one coronal slice of skull phantom was scored by six dentomaxillofacial radiologists. The authors reported that the reduction in mAs often resulted in image quality remaining within acceptable limits.¹⁶ In the relevant study, anthropometric phantom and image quality assessments were conducted by subjective scoring

of observers and QA phantom was used for quantitative tests. In the present study, both phantom types were used only for image quality estimation.

In a study, the impact of different exposure parameters on image quality and radiation dose CT system was evaluated using cadaver forearm and an orthopedic cone-beam device. Subjective and objective image quality tests were performed, and the authors reported a dose reduction of 18.9% compared to the manufacturer's recommended protocol.¹⁷ Another study investigated the image quality at different cone-beam computed tomography settings and three FOVs. CBCT scans of a cadaver head and a dry skull were scored by at least 30 observers, and results showed that the images taken at lower mA settings showed good diagnostic quality.¹⁸ While the cadaveric arm and head used in that study can be considered superior to QA or anthropometric phantoms in simulating the real patient, there are limitations regarding the repeatability and reproducibility of the imaging performed, in addition to supply and storage limitations. The two phantom types used in our study are both static and offer advantages in terms of mass production, transportation, and storage conditions.

There are numerous studies evaluating different CBCT protocols for image quality. High-dose protocols have been found to improve spatial resolution, reduce artifacts, and enhance SNR. However, despite their superior image quality, high-dose protocols are not recommended due to the associated increase in effective dose. On the other hand, low-dose protocols, when combined with noise reduction filters, are considered more beneficial for clinical applications, balancing image quality with radiation safety.^{14,19,20}

QA phantoms, anthropometric phantoms, and cadaveric specimens are used in studies with image quality elements in CBCT. While the primary role of QA phantoms is for image quality testing, dental CBCT devices are reported to require specialized QA phantoms due to their unique characteristics. However, it can be argued that an anthropometric phantom or cadaveric specimen is superior to a QA phantom in simulating a real patient. Indeed, cadaveric specimens have limitations in terms of storage and transportation. In contrast to previous anthropo-

metric phantom and image quality testing studies, quantitative calculations were made in the present study, not subjective observer scores. According to the results of this study, within its limitations, the measurements performed on anthropometric phantom slices were, to some extent, similar to the image quality tests performed with the QA phantom. However, our findings were not sufficient to fully support the use of one type of phantom over another, and future studies can be considered for more information on the subject.

One of the limitations of this study is that the imaging was performed with a single device. Moreover, this study could be improved with different FOV and other parameters. In this study, the largest FOV (13x10 cm) that does not require a vertical stitch procedure was selected. Among the slices corresponding to the three vertical heights in the anthropometric phantom, the strongest correlation with the QA phantom was found in the maxilla slice located in the center. However, the paranasal sinus and mandible regions were selected from slices closer to the upper and lower boundaries of the FOV area. Although the device supports a height of 16 cm, this is only possible with a vertical stitching procedure. In imaging with the largest FOV (13x16 cm), such centers in the vertical height will be two, not a single one, and the upper part of the lower volume and the lower part of the upper volume will overlap with one another. The vertical stitch procedure was not required for the FOV size selected in our study, and future studies can be performed with a different FOV size that require such procedure. The QA phantom utilized in this study is not the recommended QA phantom to be used in this CBCT system, and the difference in size can be considered as another limitation of this study. The relevant QA phantom is designed for use with devices that support a larger FOV, and its positioning within the device was suboptimal. This may have an impact on the results.²¹ Future studies with different QA and anthropometric phantoms that support various dental CBCT devices may be beneficial.

CONCLUSION

The development of new phantoms may address the limitations of QA phantoms, which may not meet all the criteria for assessing the quality of CBCT images. It is essential for clinicians and radiologists to

have access to cost-effective, user-friendly phantoms suited for both small and large FOVs. Results of this research support that the measurements with anthropometric phantom slices may be worth studying/considering. However, the results should be interpreted with caution. The impact of changing the imaging mode (Low Dose, Regular and Best Quality) in developing quantitative machine learning tools or additive manufacturing applications could be the subject of future research.

REFERENCES

- de las Heras Gala H, Torresin A, Dasu A, Rampado O, Delis H, Hernández Girón I, *et al.* Quality control in cone-beam computed tomography (CBCT) EFOMP-ESTRO-IAEA protocol (summary report). *Phys Med* 2017;39:67-72.
- SEDENTEXCT. European Commission, Radiation Protection N 172: Cone beam CT for dental and maxillofacial radiology. Evidence based guidelines. A report prepared by the SEDENTECT Project. 2012.
- Mihailidis DN, Stratis A, Gingold E, Carlson R, DeForest W, Gray J, *et al.* AAPM Task Group Report 261: Comprehensive quality control methodology and management of dental and maxillofacial cone beam computed tomography (CBCT) systems. *Med Phys* 2024;51:3134-64.
- Pauwels R, Stamatakis H, Manousaridis G, Walker A, Michielsen K, Bosmans H, *et al.* Development and applicability of a quality control phantom for dental cone-beam CT. *J Appl Clin Med Phys* 2011;12:245-60.
- Torgersen GR, Hol C, Møystad A, Hellén-Halme K, Nilsson M. A phantom for simplified image quality control of dental cone beam computed tomography units. *Oral Surg Oral Med Oral Pathol Oral Radiol* 2014;118:603-11.
- de Oliveira MV, Wenzel A, Campos PS, Spin-Neto R. Quality assurance phantoms for cone beam computed tomography: a systematic literature review. *Dentomaxillofac Radiol* 2017;46:20160329
- Akyea-Larbi KO, Hasford F, Inkoom S, Tetteh MA, Gyekye PK. Evaluation of organ and effective doses using anthropomorphic phantom: A comparison between experimental measurement and a commercial dose calculator. *Radiogr* 2024;30:1-5.
- Roa D, Leon S, Paucar O, Gonzales A, Schwarz B, Olguin E, *et al.* Monte Carlo simulations and phantom validation of low-dose radiotherapy to the lungs using an interventional radiology C-arm fluoroscope. *Phys Med* 2022;94:24-34.
- Kesmezacar FF, Tunçman D, Nayci AE, Günay O, Yeyin N, Üzüm G, *et al.* In-depth exploration of the radiation exposure to staff performing endoscopic retrograde cholangiopancreatography procedures (ERCP) through RANDO phantom and TLDs. *Jpn J Radiol* 2024;42:1058-66.
- Abuş F, Gürçalar A, Günay O, Tunçman D, Kesmezacar FF, Demir M. Quantification of Lens Radiation Exposure in Scopy Imaging: A Dose Level Analysis. *IJASRaR* 2024;1(1).
- Hu Y, Xu S, Li B, Inscoe CR, Tyndall DA, Lee YZ, *vd.* Improving the accuracy of bone mineral density using a multisource CBCT. *Sci Rep* 2024;14:3887.
- Nardi C, Talamonti C, Pallotta S, Saletti P, Calistri L, Cordopatri C, *et al.* Head and neck effective dose and quantitative assessment of image quality: a study to compare cone beam CT and multislice spiral CT. *Dentomaxillofac Radiol* 2017;46:20170030.
- Kadesjö N, Benchimol D, Falahat B, Näsström K, Shi X-Q. Evaluation of the effective dose of cone beam CT and multislice CT for temporomandibular joint examinations at optimized exposure levels. *Dentomaxillofac Radiol* 2015;44:20150041
- Elkhateeb SM, Torgersen GR, Arnout EA. Image quality assessment of clinically-applied CBCT protocols using a QAT phantom. *Dentomaxillofac Radiol* 2016;45: 20160075.
- Loubele M, Jacobs R, Maes F, Denis K, White S, Coudyzer W, *et al.* Image quality vs radiation dose of four cone beam computed tomography scanners. *Dentomaxillofac Radiol* 2014;37:309-19.
- Pauwels R, Seynaeve L, Henriques JCG, de Oliveira-Santos C, Souza PC, Westphalen FH, *et al.* Optimization of dental CBCT exposures through mAs reduction. *Dentomaxillofac Radiol* 2015;44: 20150108.
- Yel I, Booz C, Albrecht MH, Gruber-Rouh T, Polkowski C, Jacobi M, *vd.* Optimization of image quality and radiation dose using different cone-beam CT exposure parameters. *Eur J Radiol* 2019;116:68-75.
- Kwong JC, Palomo JM, Landers MA, Figueroa A, Hans MG. Image quality produced by different cone-beam computed tomography settings. *Am J Orthod Dentofacial Orthop* 2008;133:317-27.
- Ihlis RL, Kadesjö N, Tsilingaridis G, Benchimol D, Shi XQ. Image quality assessment of low-dose protocols in cone beam computed tomography of the anterior maxilla. *Oral Surg Oral Med Oral Pathol Oral Radiol* 2022;133:483-91.
- Abouei E, Lee S, Ford NL. Quantitative performance characterization of image quality and radiation dose for a CS 9300 dental cone beam computed tomography machine. *JMI* 2015;2:044002-044002.
- Hwang JJ, Park H, Jeong H-G, Han S-S. Change in Image Quality According to the 3D Locations of a CBCT Phantom. *PLOS ONE* 2016;11:e0153884.